Hindawi
International Journal of Antennas and Propagation
Volume 2023, Article ID 1569710, 12 pages
https://doi.org/10.1155/2023/1569710

Research Article

A Single-Layer Circularly Polarized Reflectarray Antenna with High Aperture Efficiency for Microwave Power Transmission

Huaiqing Zhang,[1] Yuxin Wang,[1] Jiapeng Wang,[1] Hui Xiao,[1] Xing Chen,[2] and Xin Wang[1]

[1]*The School of Electrical Engineering, ChongQing University, No. 174 Shazhengjie, Shapingba, Chongqing 400044, China*
[2]*The School of Electronics and Information Engineering, Sichuan University, Chengdu 610044, China*

Correspondence should be addressed to Xin Wang; wang.x@cqu.edu.cn

Received 12 October 2022; Revised 23 December 2022; Accepted 26 December 2022; Published 12 January 2023

Academic Editor: Sandeep Kumar Palaniswamy

Copyright © 2023 Huaiqing Zhang et al. This is an open access article distributed under the Creative Commons Attribution License, which permits unrestricted use, distribution, and reproduction in any medium, provided the original work is properly cited.

In this article, a single-layer circularly polarized reflectarray antenna (RA) with a linearly polarized feed is proposed for microwave power transmission. The unit cell of the reflectarray is composed of a rectangular patch surrounded by four groups of *E*-shaped structures, which feature a very low level of cross-polarization. Simulation results demonstrate that the phase of its reflection coefficient can be tuned continuously in a range of 500° by adjusting the lengths of the *E*-shaped structures. In response to a normally incident plane wave, the phase values of the reflection coefficient associated with two orthogonal linear polarization directions of the reflected wave can be tuned independently, which makes it possible to convert a linearly polarized incident wave to a circularly polarized beam. A reflectarray with 15 × 15 unit cells is fabricated and tested. The measurement results demonstrate a 3-dB axial ratio bandwidth of more than 2 GHz around the center frequency of 5.8 GHz. The measured gain value of the fabricated reflectarray is 25.4 dBi, corresponding to an aperture efficiency of 52.5%.

1. Introduction

Microwave power transmission (MPT) is a technology that uses electromagnetic waves in the microwave frequency range as the carrier to transmit power wirelessly. This technology is one of the mainstream technologies that can realize wireless power transmission over long distances with high security and high transmission power [1–3]. A microwave power transmission system is normally composed of a microwave power source, a transmitting antenna, a receiving antenna, and a rectifier circuit [4]. To improve power transmission efficiency, high-gain transmitting antennas such as parabolic antennas and microstrip array antennas are commonly employed. As a new generation of high-gain antennas, the reflectarray antenna (RA) has the advantages of high gain, low physical profile, and low-loss feed, which combine the advantages of parabolic and microstrip array antennas.

Hence, reflectarray antennas have attracted great attention in the fields of radar and satellite communication [5–8] and also have potential applications in MPT.9. Due to low loss in bad weather, reflective array antennas in the *c*-band are often designed and used. Zhang et al. present a novel broadband single-layer reflectarray with low cost for satellite communications [9]. Chakraborty et al. design a dielectric resonator wideband antenna, along with dual-band circular polarization characteristics, from 5.8 to 6.2 GHz (11.56%) for uplink *c*-band communication satellites [10]. Zhang et al. present a planar integrated folded reflectarray antenna for mobile satellite communications [11]. Besides, Slimani et al. designed an array antenna in the *c*-band for aircraft weather measurement radars to locate precipitation and estimate its type (snow, rain, etc.) [12], and Keshtkar et al. designed a circular array antenna for a *c*-band altimeter system [13]. The functions of reflective array antennas are constantly being expanded and optimized by researchers. Tahseen and

Kishk designed a circularly polarized textile reflectarray in the *c*-band to make it more flexible and portable [14]. There is also research to widen bandwidth and do compact design for *c*-band applications [15, 16]. A distributed power-amplifying capability is investigated to improve the effective isotropic radiated power of reflectarray antennas in the *c*-band [17]. It is also a hot topic of research on reconfigurable antennas regarding polarization, frequency, wave number, beam pointing, etc. [18–21].

The reflectarray proposed in [22] is linearly polarized. For applications of MPT to mobile targets such as airships, UAVs, and other aircraft, the effect of polarization mismatch needs to be taken into consideration as the attitude of these targets may change over time. To minimize the polarization mismatch effect, circularly polarized antennas are preferred for this type of application [23]. The implementation of circularly polarized reflectarray antennas is mainly based on the following two approaches.

The first approach is to use circularly polarized feed, in which phase compensation can be achieved by rotating the unit cells. With this approach, the feed antenna design is relatively complex [24–27]. The other approach is to use a linearly polarized feed. The unit cell on the array needs to have the function of converting the linearly polarized incident wave into a circularly polarized reflected wave. In [28], a new double-layer *T*-structure unit cell is proposed that is capable of obtaining polarization conversion with a phase compensation range of more than 500°. A circularly polarized reflectarray antenna with 9×9 unit cells based on this unit cell was fabricated, and a 3-dB axial ratio bandwidth of 28% was obtained. The maximum gain is 19.4 dBi at 9.5 GHz, and its aperture efficiency is 44%. An improved subwavelength Jerusalem structure with a linear phase compensation range of more than 360° is proposed in [29]. The reflectarray antenna with an aperture of 166.6 mm × 166.6 mm is designed and fabricated to achieve a 3-dB axial ratio bandwidth of 50%, and its aperture efficiency at 12.5 GHz is 46.3%. In [30], a new polarization conversion unit cell based on high-precision 3D printing technology is proposed. The unit cell obtains a phase compensation range of more than 360°. The circularly polarized reflectarray antenna is designed with genetic algorithm optimization and has a measured 3-dB axial ratio bandwidth of 19.3%.

In this paper, a single-layer circularly polarized reflectarray antenna with a linearly polarized feed is proposed. Its unit cell's reflection coefficient can be tuned continuously in a range of 500°. In response to a normally incident plane wave, the phase values of the reflection coefficient associated with two orthogonal linear polarization directions of the incident wave can be tuned independently, which makes it possible to convert a linearly polarized incident wave to a circularly polarized beam.

The rest of this article is organized as follows. In Section 2, the design and simulation of the unit cell are given, and its polarization characteristics are analyzed. In Section 2.1, a circularly polarized reflectarray antenna is designed to further verify the polarization conversion characteristics of the unit cell. In Section 2.2, the designed reflect array antenna is simulated, fabricated, and measured. Section 3 gives the conclusion of this article.

2. Design of the Unit Cell

Figure 1 shows a schematic diagram of the structure of the designed single-layer reflective unit cell. The unit cell is based on a combination of a rectangular unit cell and an *E*-shaped resonant structure. The substrate used for this unit cell is F4B ($\varepsilon_r = 2.65$, $\tan\delta = 0.002$). The length of the dielectric layer $L = 25$ mm is about $0.48\lambda_0$, where λ_0 is the wavelength of microwaves in vacuum at 5.8 GHz. The substrate thickness of the unit cell is $h = 2$ mm, and an air layer of thickness $h_a = 4$ mm is added to the bottom of the dielectric layer to make the reflection phase curve smooth. The dimensions of the main parameters of the unit cell are shown in Table 1.

The designed unit cell is subjected to full-wave simulation with periodic boundary conditions in CST. Figure 2 shows the variation of the reflection phase as a function of the air layer thickness at the center frequency of 5.8 GHz. It shows that it is significant to add an air layer to the unit cell. Besides, it is found that the thickness of the air layer has a significant effect on the phase characteristic curve. With both the range and linearity of the phase variation taken into account, $h_a = 4$ mm is selected as the optimal thickness of the air layer.

Figure 3 shows the reflection phase variation curves of the proposed unit cell at different frequencies. When the dimension parameter l_x along the *x*-direction is varied from 7 mm to 13 mm, the phase varies in the range of about 500° at 5.8 GHz. Similar reflection phase variation characteristics are observed in the frequency range from 4.5 GHz to 6.5 GHz, all with the phase compensation range being more than 360°. This enables the reflectarray based on the proposed unit cell design to operate over a wide frequency range. We get the reflection magnitude plot as a function of length at the frequencies of 4.5 GHz, 5.8 GHz, and 6.5 GHz, as shown in Figure 4. It can be seen that size and frequency have almost no effect on the amplitude.

Figure 5 represents the effect of the size of the unit cell in the *y* direction on the *x*-polarized reflection performance of the unit cell. The maximum variation of the phase curve for different l_y is about 20°, indicating a low cross-polarization coupling level. To further verify the conclusion, the electric fields induced on the unit cell surface were analyzed at 5.8 GHz. It can be found that, under the *x*-polarized electric field excitation, the induced electric field intensity generated in the *x*-axis direction on the unit cell surface is much larger than that in the *y*-direction, which further indicates that the cross-polarization coupling is very weak.

The evolution of the unit cell is shown in Figure 6. The linear-circular polarization conversion (LCPC) unit cell is derived from the first *E*-shape (Single-E) structure, which is designed by the theory of LCPC elaborated in the next part. Here is a brief explanation: the linear polarization wave incident at an angle of 45 degrees between the *x*-axis

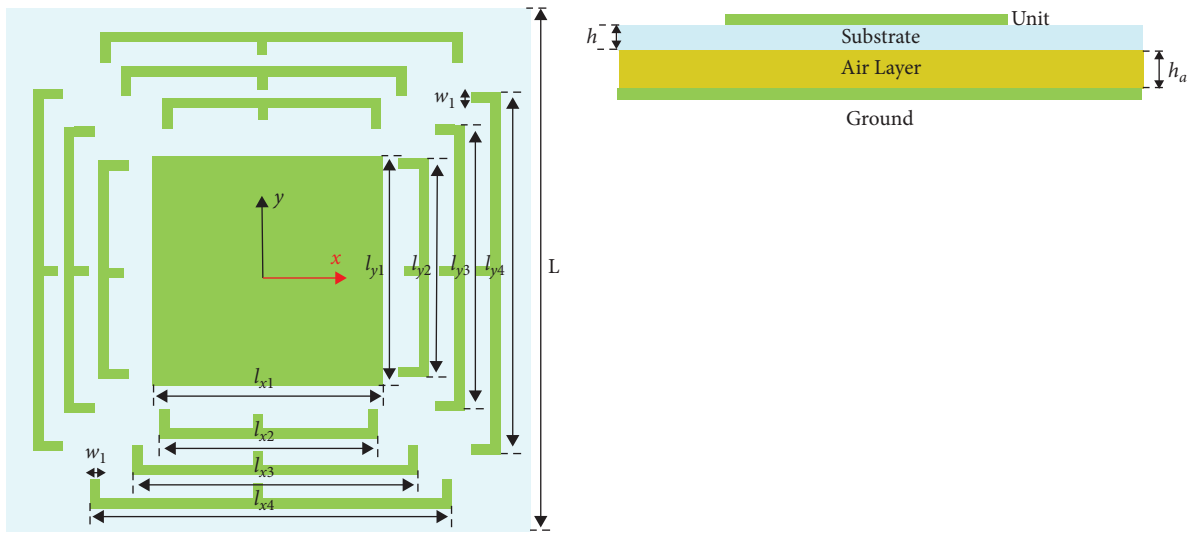

Figure 1: (a) Top view of the unit cell. (b) Side view of the unit cell.

Table 1: Parameter values of unit cell geometry.

lx	lx1	lx2	lx3	lx4	h
7–13 cm	0.8*lx	0.9*lx	1.2*lx	1.5*lx	2 mm
ly	ly1	ly2	ly3	ly4	$w1$
7–13 cm	0.8*ly	0.8*ly	0.8*ly	0.8*ly	0.5 mm

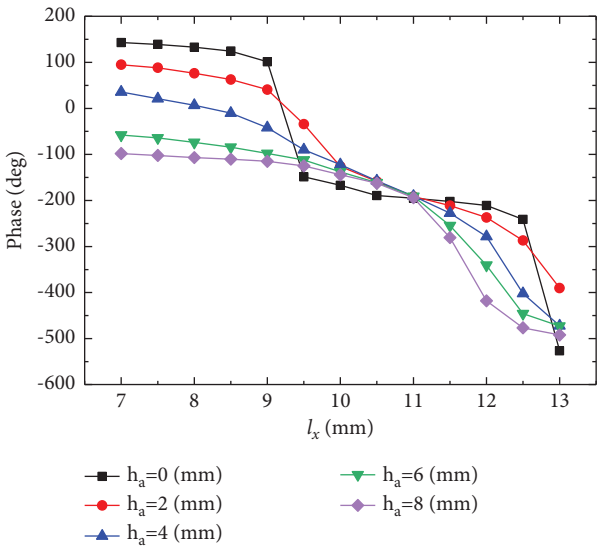

Figure 2: Optimization of air layer thickness.

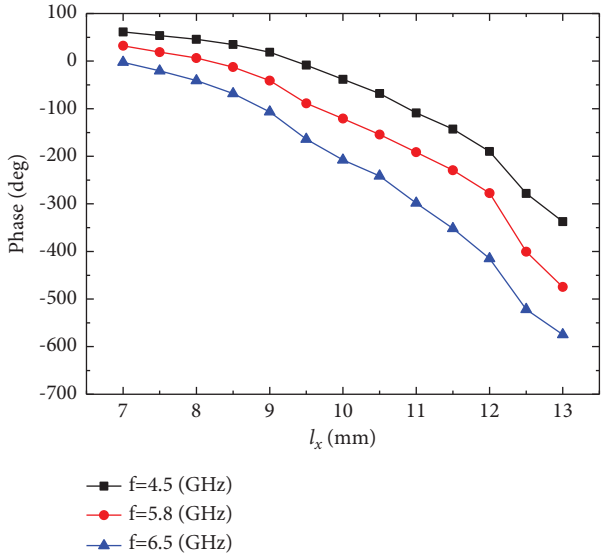

Figure 3: Reflected phase characteristic curve.

and y-axis can be effectively converted into a reflection wave with the same reflection coefficient in the x-direction and y-direction, which also has a relatively high gain.

However, the structure cannot achieve a wide range of reflection phase bands. Therefore, we consider adding an E-frame to the unit cell to widen the range of reflection phase shifts of the unit cell without changing the circular polarization characteristics. We simulate the phase response curves versus the length at 5.8 GHz, as shown in Figure 7. It is shown that the bandwidth can be significantly improved by adding E-frames.

As shown in Figure 7, within the size range of 7–13 mm, for Single-E and Double-E structures, the range of phase is 181 and 304, respectively, less than 360, which does not meet the requirements. The phase range of the Quadruple-E structure is too large to achieve the requirement of a smooth curve. For the Triple-E structure, the maximum slope of its phase response curve decreases to 101. This means that more resonance points are near 5.8 GHz, there is more than 40% improvement compared with the Quadruple-E structure, and the phase range is also extended from 304° to nearly 500° compared with the Double-E structure.

We further analyze the role of the E-shape resonant structure from the perspective of the surface electric field of the unit cell, as shown in Figure 8. It can be concluded that

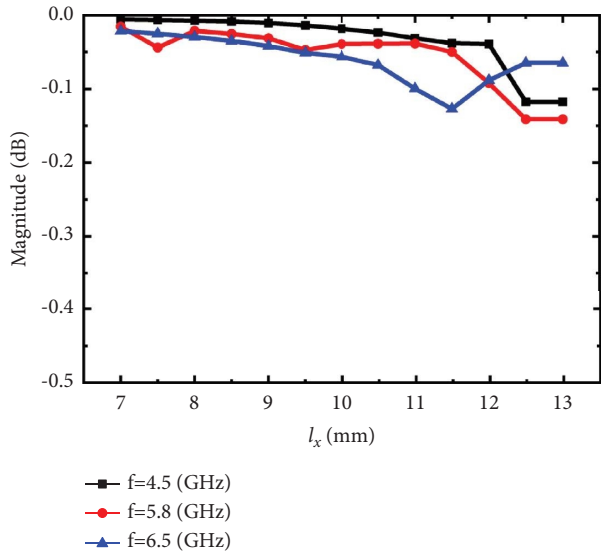

Figure 4: Reflected magnitude characteristic curve.

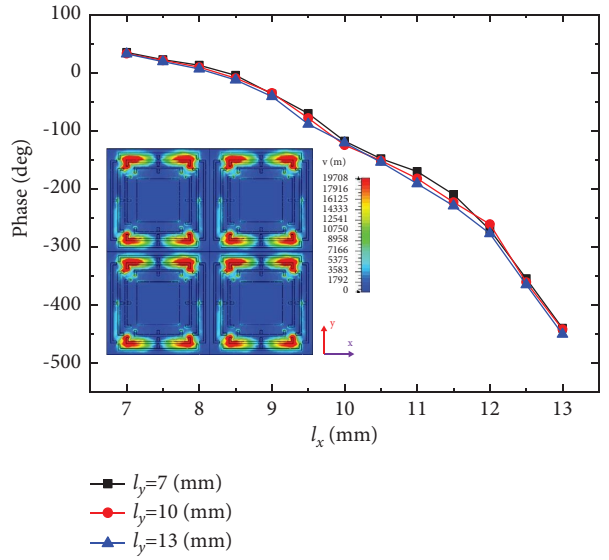

Figure 5: Surface electric field and phase characteristic curves of the unit cell.

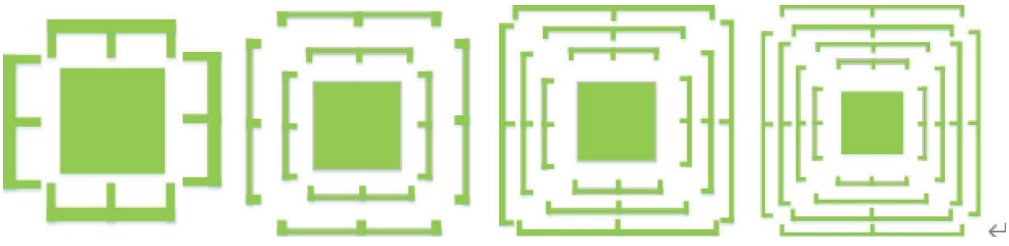

Figure 6: Evolution of the unit cell.

the induced electric field polarized in the x-direction is shifted from the outermost E-shape resonance structure to the innermost E-shape resonance structure as the frequency increases, which proves that the multi-E-shape resonance structure is effective.

2.1. Design of Circularly Polarized Reflectarray Antenna. Based on the design and analysis of the unit cell in the previous section, a 15×15 left-handed circularly polarized reflectarray antenna is designed in order to further verify its line polarization to circular polarization conversion

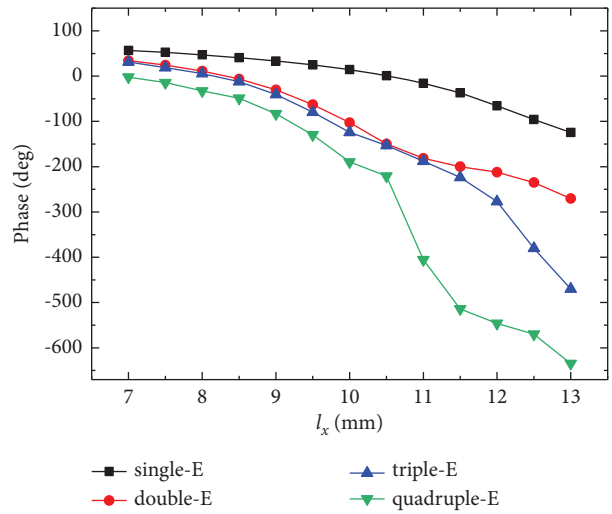

Figure 7: Reflection phases versus the size of the unit cell of 0° for the four types of the *E*-shape structure.

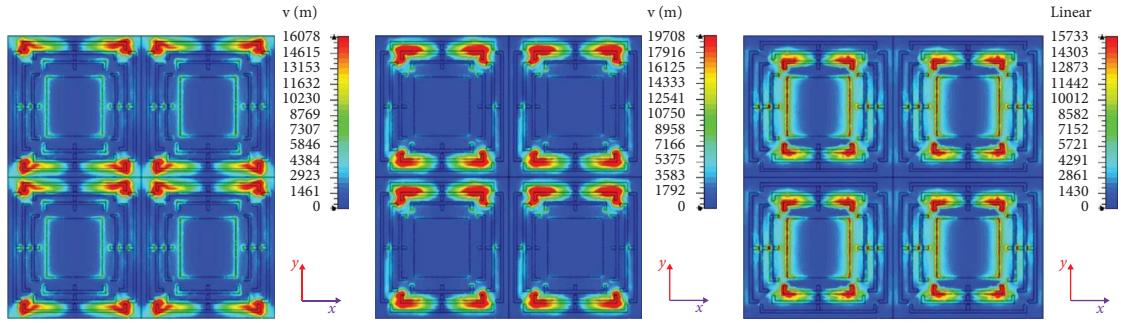

Figure 8: Surface electric field at (a) 4.5 GHz, (b) 5.8 GHz, and (c) 6.5 GHz.

characteristics. The aperture of the reflectarray antenna is 375 mm × 375 mm, and its electrical size is $(7.25\lambda_0)^2$. The feed is positioned 20° off the normal direction. The focal diameter ratio of the reflectarray antenna is $F/D = 1.3$, and its aperture side length is $D = 375$ mm. The electromagnetic wave radiated from the feed is incident along the $(-z)$ direction, and its electric field polarization direction makes an angle θ with the x-axis. When $\theta = 45°$, the electric field of the incident wave can be expressed as

$$\mathbf{E}^{\mathbf{in}} = \frac{\sqrt{2}}{2}[\mathbf{u}, \mathbf{v}][1, 1]^T, \tag{1}$$

where $\mathbf{u}$ and $\mathbf{v}$ denote the horizontal and vertical polarization direction unit cell vectors, respectively. When the phase of the reflection of the y-polarized wave is 90° ahead of that of the x-polarized wave, the reflection coefficient matrix of the unit cell can be expressed as

$$R = \begin{bmatrix} 1 & 0 \\ 0 & j \end{bmatrix}. \tag{2}$$

Then, the electric field expression of the reflected wave after the unit cell reflection is

$$\mathbf{E}^{\mathbf{re}} = \frac{\sqrt{2}}{2}[\mathbf{u}, \mathbf{v}][1, j]^T, \tag{3}$$

which represents a left-handed circularly polarized wave. Therefore, in order to realize the conversion from a linearly polarized incident wave to a left-handed circularly polarized outgoing wave, the phase compensation in the y-axis direction of the unit cell needs to be 90° more than in the x-axis direction. The value of phase compensation $\varphi_x^n(m,n)$ in the x-direction of the unit cell is calculated as [17]

$$\varphi_x^n(m,n) = k_0\left(r_{mn} - \sin\theta_b\left(x_m\cos\varphi_b + y_n\sin\varphi_b\right)\right) + \varphi_0, \tag{4}$$

where $k_0 = (2\pi/\lambda)$ is the free space propagation constant and r_{mn} is the distance from the feed phase center to the unit cell located at (x_m, y_n). The coordinates (θ_b, φ_b) are the expected azimuth and pitch angles of the main beam, respectively. φ_0 indicates the phase constant. Then, the phase compensation value $\varphi_y^n(m,n)$ in the y-axis direction can be expressed as

$$\varphi_y^n(m,n) = \varphi_x^n(m,n) + 90°. \tag{5}$$

We conducted simulations of cell characteristics before setting up the reflectarray (RA). From the analysis, it is known that the reflection coefficients r_x and r_y need to be as equal as possible and provide a phase difference of $\Delta\varphi = \varphi_y^{\mathrm{rn}}(m,n) - \varphi_x^{\mathrm{rn}}(m,n) = 2m\pi \pm (\pi/2)$ (m is an integer) for the function of linear-circular polarization conversion (LCPC). "–" and "+" denote the left and right circular polarizations, respectively [31].

As shown in Figure 9, in the frequency band of 4.2–6.8 GHz, the reflection coefficients r_x and r_y exhibit approximately equal intensities. This implies that the incident wave can be converted into x- and y-polarization components with the same intensity. Furthermore, in the same frequency range, the phase difference $\Delta\varphi$ is approximately 90° for the reflected wave, which is necessary for right circular polarization. The related geometry parameters are $lx = 8$ mm and $ly = 13$ mm.

The realization of LCPC can be indicated by the ellipticity and axis ratio. The normalized ellipticity of $E = (2|r_x||r_y|\sin(\Delta\varphi)/(|r_x|^2 + |r_y|^2))$ can be defined to estimate the effects of the polarization conversion. An ideal circularly polarized wave has an ellipticity of 1. When $E = -1$, the reflected wave is right-circularly polarized. The reflected wave has left circular polarization when $E = +1$. An ellipticity larger than 0.90 is regarded to correspond to a circularly polarized wave [32]. It shows the relationship between ellipticity and frequency in Figure 10. The ellipticity is close to 1 in the frequency band of 4.4–6.1 GHz, which confirms that the reflected wave is left-circularly polarized. The axis ratio $E = (2|r_x||r_y|\sin(\Delta\varphi)/(|r_x|^2 + |r_y|^2))$ is also used to evaluate the degree of circular polarization [33]. Figure 10 shows the calculated results. The axis ratios of the reflected wave are lower than 3 dB in the wide frequency band of 4.4–16.5 GHz, which indicates that the designed metasurface provides a good performance in LCPC.

Then, we set up the array based on the unit cell characteristics. According to equations (4) and (5), the phase distributions of the unit cell in the x-axis and y-axis polarization directions can be calculated in MATLAB, respectively, as shown in Figures 11(a) and 11(b).

The phase distribution maps in the x and y directions in Figure 11 are transformed into the size distribution of the unit cells on the array in the x and y directions by the phase curve at 5.8 GHz in Figure 3, as shown in Figure 12.

2.2. Experiment and Measurement Results of the Reflectarray Antenna. In this section, a circularly polarized reflectarray antenna (RA) with a unit cell number of 15 × 15 is simulated, fabricated, and measured. The corresponding RA model is established using MATLAB in conjunction with CST, and the feed horn antenna model is established, as shown in Figure 13. The designed RA is verified in CST using full-wave simulation. The 3-D radiation of RA is shown in Figure 14, whose E field and H field radiation patterns are shown in Figures 15(a) and 15(b), respectively. From the measured radiation patterns, it can be concluded that the 3 dB main beamwidth is 15°-16°. The peak gain value was 25.4 dBi. The

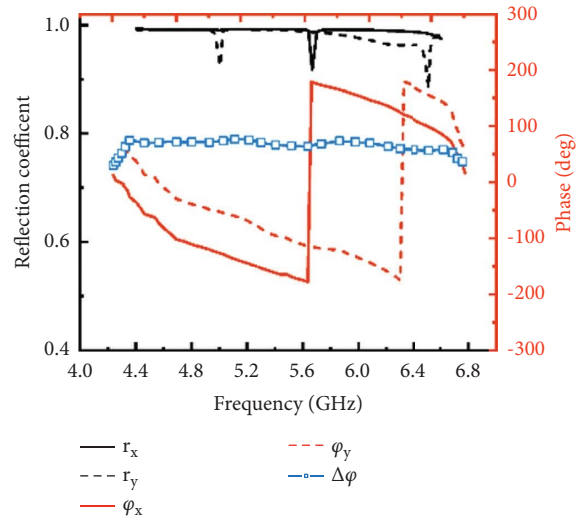

Figure 9: Simulated reflection coefficients and phases of the unit cell.

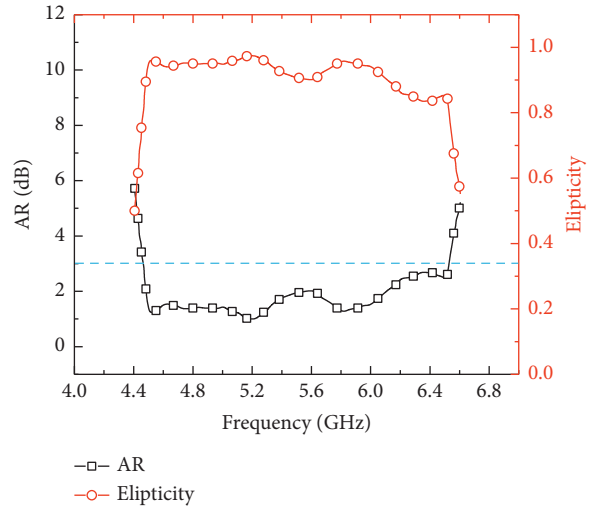

Figure 10: Simulated ellipticity and axis ratio.

side-lobe levels of the E-pattern and H-pattern are 5.6 dBi and 6.3 dBi, respectively.

The fabricated RA with the measurement settings is shown in Figure 16. The simulated and measured gain patterns in the x-z plane at frequencies of 4.5 GHz, 5.8 GHz, and 6.5 GHz are illustrated in Figure 17. It can be found that the cross-polarization level of the RA is below −15 dB at all three frequencies.

Figure 18 plots the axial ratio (AR) of the simulated and measured results of the RA. It can be found that the RA has an axial ratio below 3 dB in the frequency range from 4.45 to 6.54 GHz, and its 3-dB AR bandwidth is about 38%. It shows that the RA is a circularly polarized antenna in this frequency range.

Figure 19 gives the simulated and measured gain plots of this RA at different frequencies. The measured gain of the antenna is 25.4 dBi at the center frequency of

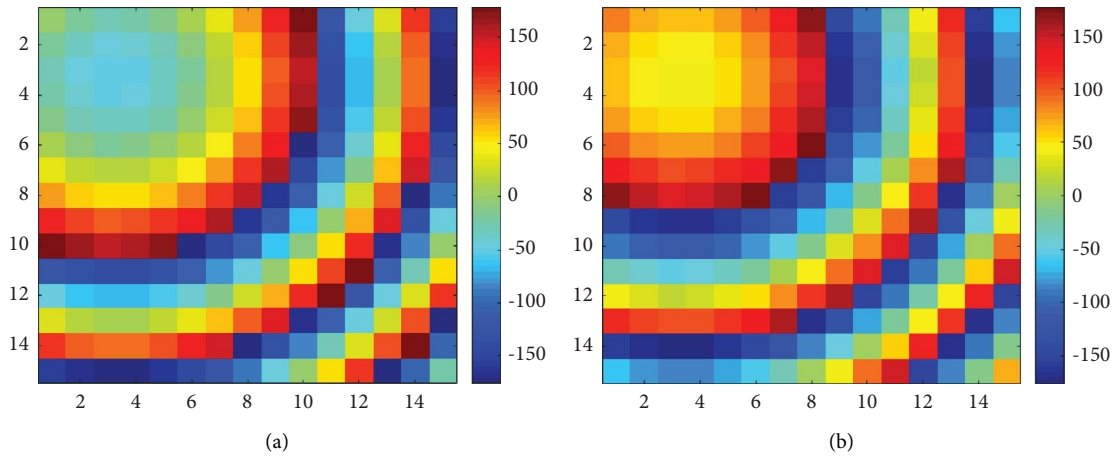

Figure 11: Unit cell phase compensation value along (a) the x-polarization direction and (b) the y-polarization direction.

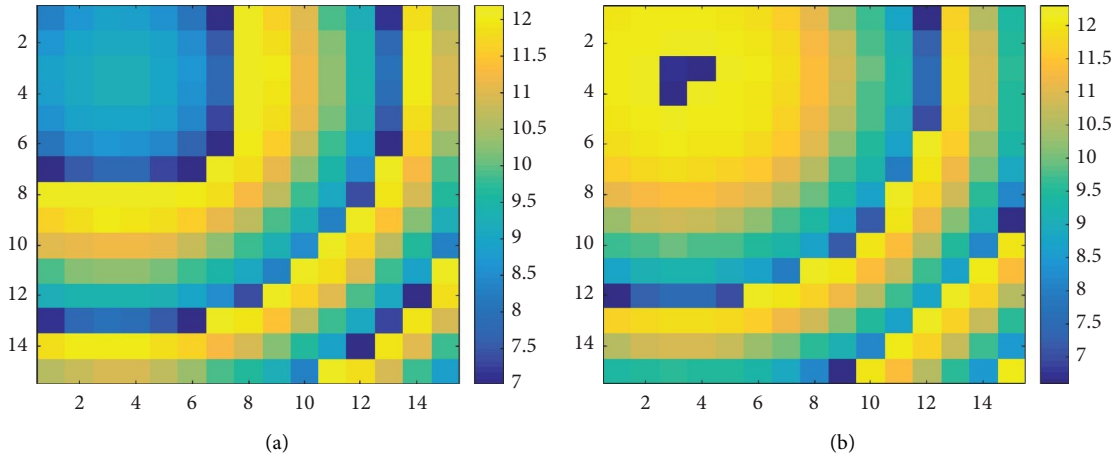

Figure 12: Unit cell size distribution: (a) the length parameter lx and (b) the length parameter ly.

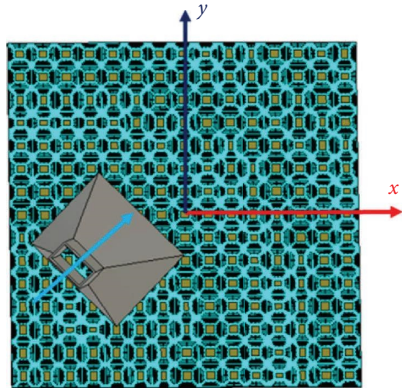

Figure 13: Reflectarray antenna simulation model diagram.

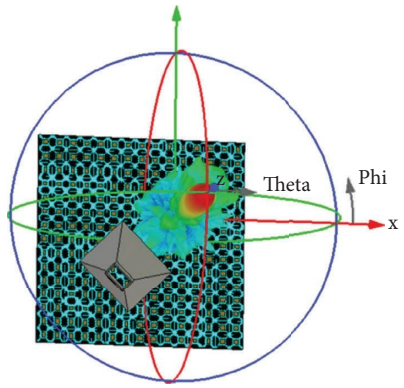

Figure 14: Simulation of a 3D radiation pattern.

5.8 GHz. According to the definition of the aperture efficiency $\varepsilon = G\lambda^2/(4\pi A)$, where A is the physical aperture area of the antenna, the aperture efficiency of this RA is calculated to be 52.5%. Its 1-dB gain bandwidth is 17.1% (from 5.28 to 6.27 GHz). Also, its axis ratio is below 3 dB in the 1-dB gain bandwidth range.

Besides, we conduct experiments to verify its availability in MPT. We use a 5.8 GHz horn antenna and RA as the transmitting antennas, respectively, and another horn antenna as the receiving antenna. Change the distance between the receiving antenna and the transmitting antenna from 1.5 m to 9 m, measure the power received by the receiving

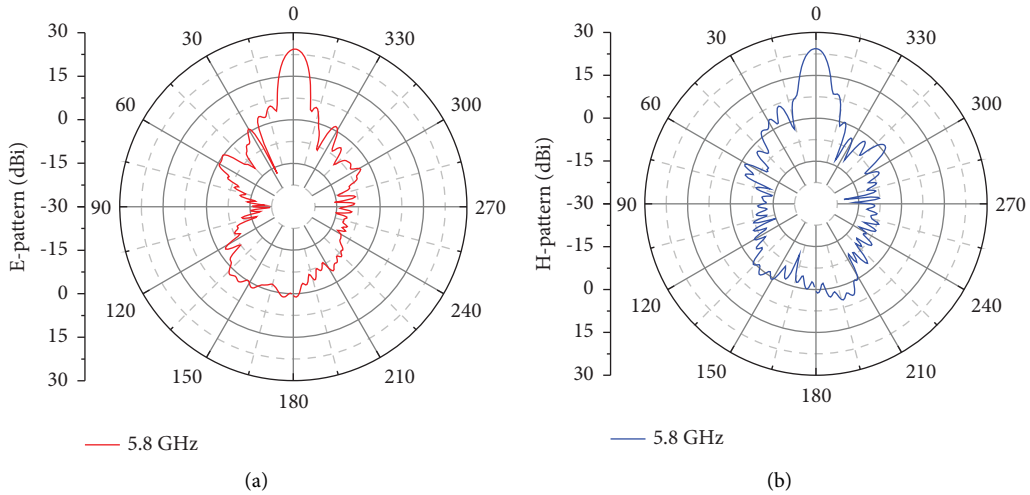

Figure 15: *E*-field and *H*-field radiation patterns.

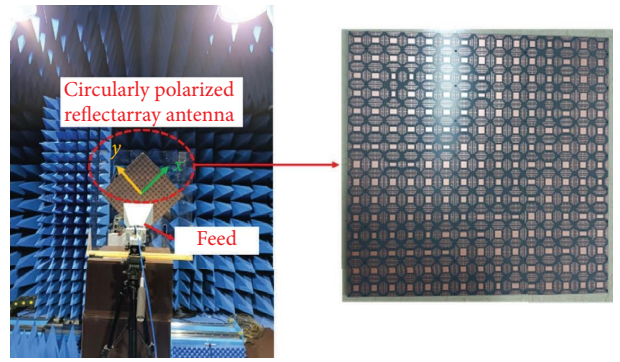

Figure 16: Reflect array antenna physical measurement diagram.

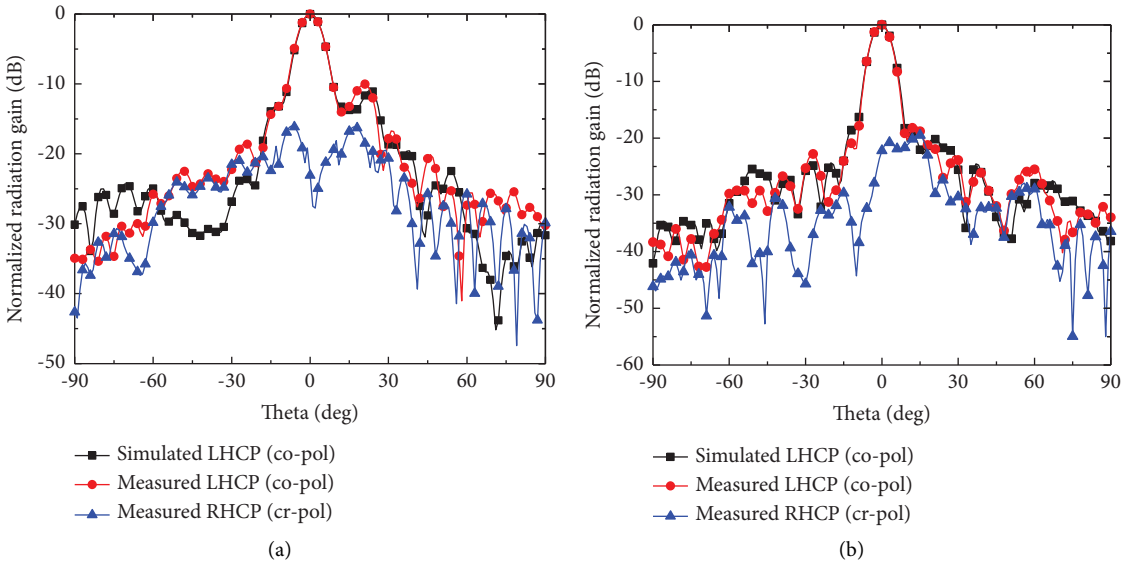

Figure 17: Continued.

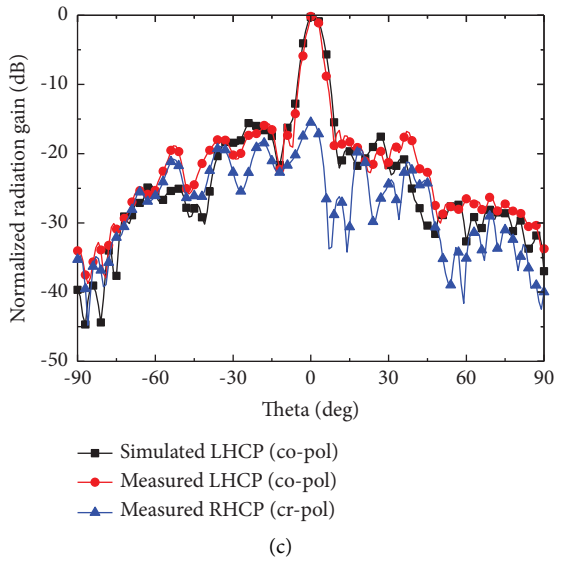

Figure 17: The normalized gain pattern of the reflectarray antenna at (a) 4.5 GHz, (b) 5.8 GHz, and (c) 6.5 GHz.

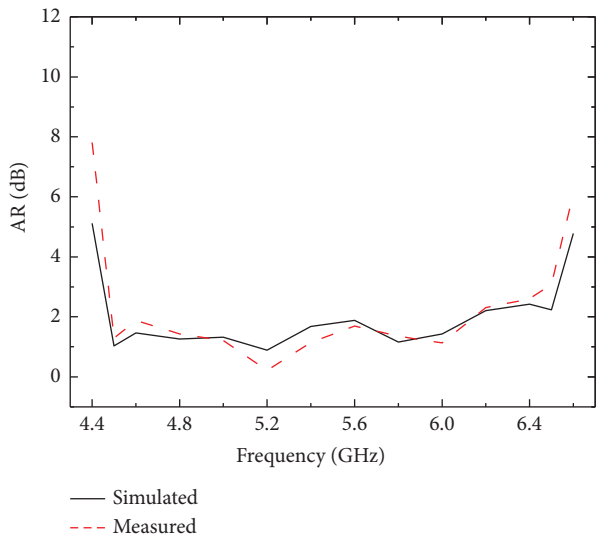

Figure 18: Comparison of simulation and measurement of axial ratio.

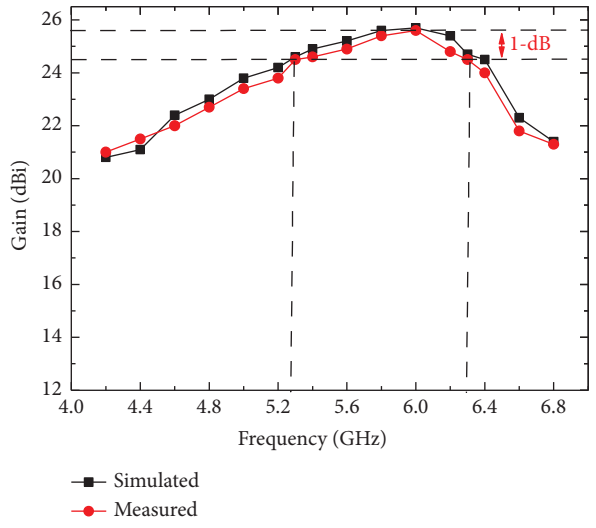

Figure 19: Gain versus frequency curve.

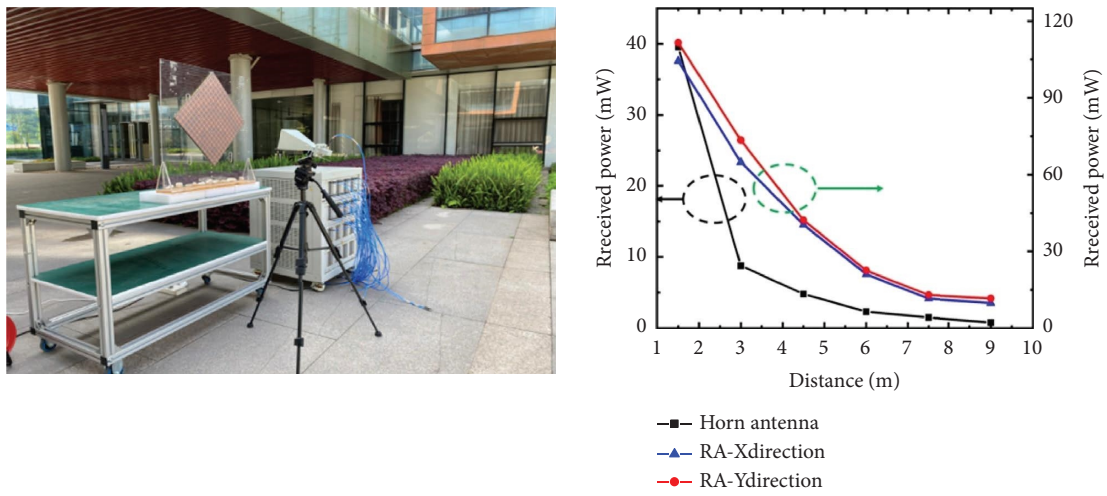

Figure 20: Power transmission measurement.

Table 2: Comparison with other literature.

References	Center frequency (GHz)	Feeder polarization	Phase range (°)	Aperture size	3-dB AR BW (%)	Aperture efficiency (%)	No. of layers
[27]	10	LP	500	$(4.2\lambda)^2$	28	44	2
[28]	12	LP	400	$(6.7\lambda)^2$	50	46.3	1
[29]	30	LP	360	$(11.25\lambda)^2$	19.3	17	1
[34]	9.4	LP	325	$(7.5\lambda)^2$	8.6	21.8	1
This work	5.8	LP	500	$(7.25\lambda)^2$	38	52.5	1

antenna, and draw the curve between the distance and the received power, as shown in Figure 20. It can be found that the received power using RA changes from 13 mW to 106 mW based on the distance, which is significantly greater than that using the horn antenna as the transmitting antenna. Moreover, we rotate the angle of the receiving antenna, which is equivalent to a change in the direction of wave polarization. It can be measured that the received power in the x-direction and y-direction are similar, which proves its availability to minimize the effect of polarization mismatch in MPT.

In Table 2, the performance of the designed RA is also compared with those in several recently published pieces of literature. Overall, the proposed reflectarray design in this paper exhibits superior performance when both the phase range and aperture efficiency are taken into consideration.

3. Conclusion

In this article, a single-layer circularly polarized reflectarray antenna (RA) with a center frequency of 5.8 GHz is proposed. The unit cell structure of the reflectarray features a linear phase coverage of more than 500° and a low cross-polarization in the reflected waves. To verify the polarization conversion characteristics of the unit cell, a 15×15 RA is fabricated, using a linear-polarization horn antenna as the feed. The experimental results show that the 3-dB bandwidth of the proposed RA is about 38% (4.45 GHz–6.54 GHz). Meanwhile, the antenna gain is 25.8 dBi at 5.8 GHz, and its aperture efficiency is 52.5%. Compared with the published literature of the same type, the proposed circularly polarized reflector array antenna is simple to process with a single-layer structure and has a wide 3-dB AR bandwidth and high aperture efficiency, which makes it potentially useful for microwave power transmission.

Data Availability

The data used to support the findings of this study are included within the article.

Conflicts of Interest

The authors declare that there are no conflicts of interest.

Acknowledgments

This work was supported by the Chengdu-Chongqing Double-city Economic Circle Construction Technology Innovation Project (Grant no. KJCXZD2020001), Chongqing Technology Innovation and Application Development Project (Grant no. cstc2019jscx-dxwtBX0001), and the Science and Technology Research Program of the Chongqing Municipal Education Commission (Grant no. KJZD-K202000103). This work was supported in part by the Graduate Research and Innovation Foundation of Chongqing (Grant no. CYS22027).

References

[1] Y. Dong, S. Dong, Y. Wang et al., "Focused microwave power transmission system with high-efficiency rectifying surface," *IET Microwaves, Antennas & Propagation*, vol. 12, no. 5, pp. 808–813, 2018.

[2] P. E. Glaser, "Power from the Sun: its Future," *Science*, vol. 162, no. 3856, pp. 857–861, 1968.

[3] N. Shinohara, *Theory Of WPT: Wireless Power Transfer via Radiowaves*, Wiley, New York, NY, USA, 2014.

[4] X. Yi, Q. Chen, S. Hao, and X. Chen, "An efficient 5.8GHz microwave wireless power transmission system," *International Journal of RF and Microwave Computer-Aided Engineering*, vol. 32, no. 5, Article ID e23094, 2022.

[5] C. Han, Y. Zhang, and Q. Yang, "A broadband reflectarray antenna using Triple Gapped Rings with Attached phase-Delay lines," *IEEE Transactions on Antennas and Propagation*, vol. 65, no. 5, pp. 2713–2717, 2017.

[6] H. Bodur and S. Çimen, "Reflectarray antenna design with double cutted ring element forX-band applications," *Microwave and Optical Technology Letters*, vol. 62, no. 10, pp. 3248–3254, 2020.

[7] S. V. Hum and J. Perruisseau-Carrier, "Reconfigurable reflectarrays and array Lenses for Dynamic antenna beam Control: a Review," *IEEE Transactions on Antennas and Propagation*, vol. 62, no. 1, pp. 183–198, 2014.

[8] C. Han, Y. Zhang, and Q. Yang, "A novel single-layer Unit structure for broadband reflectarray antenna," *IEEE Antennas and Wireless Propagation Letters*, vol. 16, pp. 681–684, 2017.

[9] K. Zhang, J. Li, G. Wei, J. Xu, and S. Gao, "Low-cost Single-Layer Broadband Reflectarray for Satellite Communications," in *Proceedings of the 2013 Loughborough Antennas & Propagation Conference*, pp. 78–83, Loughborough, England, November 2013.

[10] P. Chakraborty, U. Banerjee, A. Saha, and A. Karmakar, "A compactUltra Wideband dielectric resonator antenna with dual-band circular polarization characteristics," *International Journal of RF and Microwave Computer-Aided Engineering*, vol. 31, no. 4, Article ID e22577, 2021.

[11] C. Zhang, Y. Wang, F. Zhu et al., "A planar integrated folded reflectarray antenna with circular polarization," *IEEE Transactions on Antennas and Propagation*, vol. 65, no. 1, pp. 385–390, 2017.

[12] A. Slimani, S. D. Bennani, A. El Alami, and J. Terhzaz, "Ultra wideband planar microstrip array antennas for C-band aircraft weather radar applications," *International Journal of Antennas and Propagation*, vol. 2017, Article ID 2346068, 8 pages, 2017.

[13] A. Keshtkar, A. Keshtkar, and A. R. Dastkhosh, "Circular microstrip patch array antenna for C-band altimeter system," *International Journal of Antennas and Propagation*, vol. 2008, Article ID 389418, 7 pages, 2008.

[14] M. M. Tahseen and A. A. Kishk, "C-Band flexible and portable circularly polarized textile-reflectarray (TRA)," pp. 87-88, 2017.

[15] P. Dawar, N. S. Raghava, and A. De, "UWB Metamaterial-Loaded antenna for C-band applications," *International Journal of Antennas and Propagation*, vol. 2019, Article ID 6087039, 13 pages, 2019.

[16] C. Yu, T. Xu, and C. Liu, "Design of a novel UWB omnidirectional antenna using particle Swarm optimization," *International Journal of Antennas and Propagation*, vol. 2015, Article ID 303195, 7 pages, 2015.

[17] X. Yang, S. Xu, F. Yang, M. Li, H. Fang, and Y. Hou, "A distributed power-amplifying reflectarray antenna for EIRP boost applications," *IEEE Antennas and Wireless Propagation Letters*, vol. 16, pp. 2742–2745, 2017.

[18] Y. Li and A. Abbosh, "Reconfigurable reflectarray antenna using single-layer radiator controlled by PIN diodes," *IET Microwaves, Antennas & Propagation*, vol. 9, no. 7, pp. 664–671, 2015.

[19] C. Zhang, G. Wei, J. Li, F. Qin, and S. Gao, "Dual-polarized Unit-Cell Element for Wide-Angle Electronically Beam-Scanning Reflectarray," in *Proceedings of the 2014 Loughborough Antennas and Propagation Conference*, pp. 457–460, Loughborough, England, November 2014.

[20] T. Makdissy and I. Hassoun, "Coupled slots varactor-tuned unit cell for single linear polarization reflectarrays at c-band," in *Proceedings of the 2020 IEEE International RF and Microwave Conference*, pp. 1–4, Kuala Lumpur, Malaysia, December 2020.

[21] X. Yang, S. Xu, F. Yang et al., "A mechanically reconfigurable reflectarray with Slotted patches of tunable height," *IEEE Antennas and Wireless Propagation Letters*, vol. 17, no. 4, pp. 555–558, 2018.

[22] H. Zhang, J. Wang, H. Xiao, and X. Wang, "A broadband reflectarray antenna for microwave power transmission," *Advances in Astronautics Science and Technology*, vol. 5, no. 1, pp. 65–71, 2022.

[23] D. M. Nguyen, N. D. Au, and C. Seo, "A microwave power transmission system using Sequential phase ring antenna and inverted Class F Rectenna," *IEEE Access*, vol. 9, pp. 134163–134173, 2021.

[24] X. Yang, S. Xu, F. Yang et al., "A broadband high-efficiency reconfigurable reflectarray antenna using Mechanically Rotational elements," *IEEE Transactions on Antennas and Propagation*, vol. 65, no. 8, pp. 3959–3966, 2017.

[25] M. Y. Zhao, G. Q. Zhang, X. Lei, J. M. Wu, and J. Y. Shang, "Design of new single-layer Multiple-resonance broadband circularly polarized reflectarrays," *IEEE Antennas and Wireless Propagation Letters*, vol. 12, pp. 356–359, 2013.

[26] L. Zhang, S. Gao, Q. Luo, W. Li, Y. He, and Q. Li, "Single-layer wideband circularly polarized high-efficiency reflectarray for satellite communications," *IEEE Transactions on Antennas and Propagation*, vol. 65, no. 9, pp. 4529–4538, 2017.

[27] F. Wu, J. Wang, Y. Zhang, W. Hong, and K. M. Luk, "A broadband circularly polarized reflectarray with Magneto-electric Dipole elements," *IEEE Transactions on Antennas and Propagation*, vol. 69, no. 10, pp. 7005–7010, 2021.

[28] L. Ren, Y. Jiao, F. Li, J. Zhao, and G. Zhao, "A dual-layer T-shaped element for broadband circularly polarized reflectarray with linearly polarized feed," *IEEE Antennas and Wireless Propagation Letters*, vol. 10, pp. 407–410, 2011-01-01 2011.

[29] G. B. Wu, S. W. Qu, S. Yang, and C. H. Chan, "Broadband, single-layer dual circularly polarized reflectarrays with linearly polarized feed," *IEEE Transactions on Antennas and Propagation*, vol. 64, no. 10, pp. 4235–4241, 2016.

[30] B. Li, C. Y. Mei, Y. Zhou, and X. Lv, "A 3-D-printed wideband circularly polarized dielectric reflectarray of cross-shaped element," *IEEE Antennas and Wireless Propagation Letters*, vol. 19, no. 10, pp. 1734–1738, 2020.

[31] Y. Jiang, L. Wang, J. Wang, C. N. Akwuruoha, and W. Cao, "Ultra-wideband high-efficiency reflective linear-to-circular polarization converter based on metasurface at terahertz frequencies," *Optics express*, vol. 25, no. 22, pp. 27616–27623, 2017.

[32] S. Quader, J. Zhang, M. R. Akram, and W. Zhu, "Graphene-based high-efficiency broadband tunable linear-to-circular polarization converter for terahertz waves," *IEEE journal of selected topics in quantum electronics*, vol. 26, no. 5, pp. 1–8, 2020.

[33] Y. Li, J. Zhang, S. Qu et al., "Achieving wide-band linear-to-circular polarization conversion using ultra-thin bi-layered metasurfaces," *Journal of applied physics*, vol. 117, no. 4, Article ID 044501, 2015.

[34] P. Nayeri, Y. Fan, and A. Z. Elsherbeni, *Analysis and design of reflectarray elements*, Wiley-IEEE Press, New York, NY, USA, 2018.